Supplementary Material

Autophagy supports generation of cells with high CD44 expression via modulation of oxidative stress and Parkin-mediated mitochondrial clearance

Whelan KA, et al.

Supplementary Table S1 Effects of autophagy inhibition on TE11 xenograft tumor morphology

Treatment	Tumor ID	Cystic Changes*	Involution#
Vehicle	1	-	-
Vehicle	2	-	-
Vehicle	3	-	+
Vehicle	4	-	-
Vehicle	5	+	-
Vehicle	6	-	-
HCQ	1	+	-
HCQ	2	+	-
HCQ	3	+	-
HCQ	4	+	-
HCQ	5	+	-
HCQ	6	+	-
HCQ	7	+	-
HCQ	8	-	-
Lys05	1	+	-
Lys05	2	-	-
Lys05	3	-	+
Lys05	4	+	-
Lys05	5	-	+
Lys05	6	+	-
Lys05	7	-	+
Lys05	8	-	+

HCQ, hydroxychloroquine

**Cystic changes* include the presence of empty areas surrounded by tumor cells with or without proteinaceous debris

#*Involution* is defined as necrotic areas comprised of tumor cell debris and inflammatory cell infiltrates

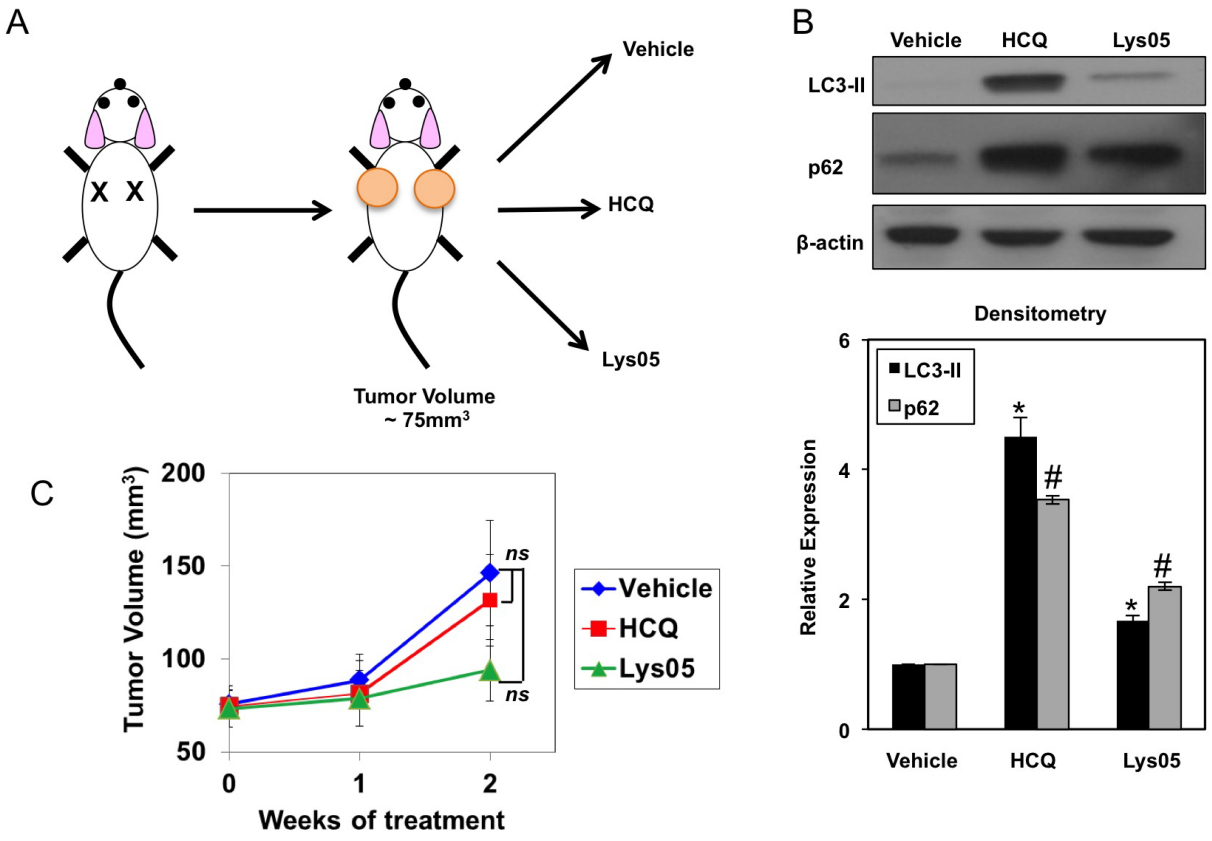

Supplementary Figure S1. Effects of pharmacological autophagy inhibition upon ESCC tumor volume and histology. (A) Schematic of xenotransplantation study. Immunocompromised mice were injected with TE11 ESCC cells and tumor volume was monitored. When tumors reached ~75 mm^3, mice were assigned to treatment groups as indicated. HCQ (60 mg/kg), Lys05 (20 mg/kg) or vehicle control were delivered via *i.p.* injection according to a 3 days on/2 days off regimen for 14 days. (B) Tumor tissue was evaluated for expression of indicated protein via immunoblotting with β-actin as a loading control as shown in bar diagram (mean ± sem). Densitometry determined level of indicated proteins relative to β-Actin. *, p<0.05 vs. vehicle for LC3; #, p<0.05 vs. vehicle for p62; ANOVA with Tukey's post-hoc test; (n=3 animals/group). (C) Average tumor volume in each group at indicated time points. *ns*, not significant; repeated measures ANOVA; (n=8 animals/group). (D) Representative H&E images. Scale bar, 100 μm.

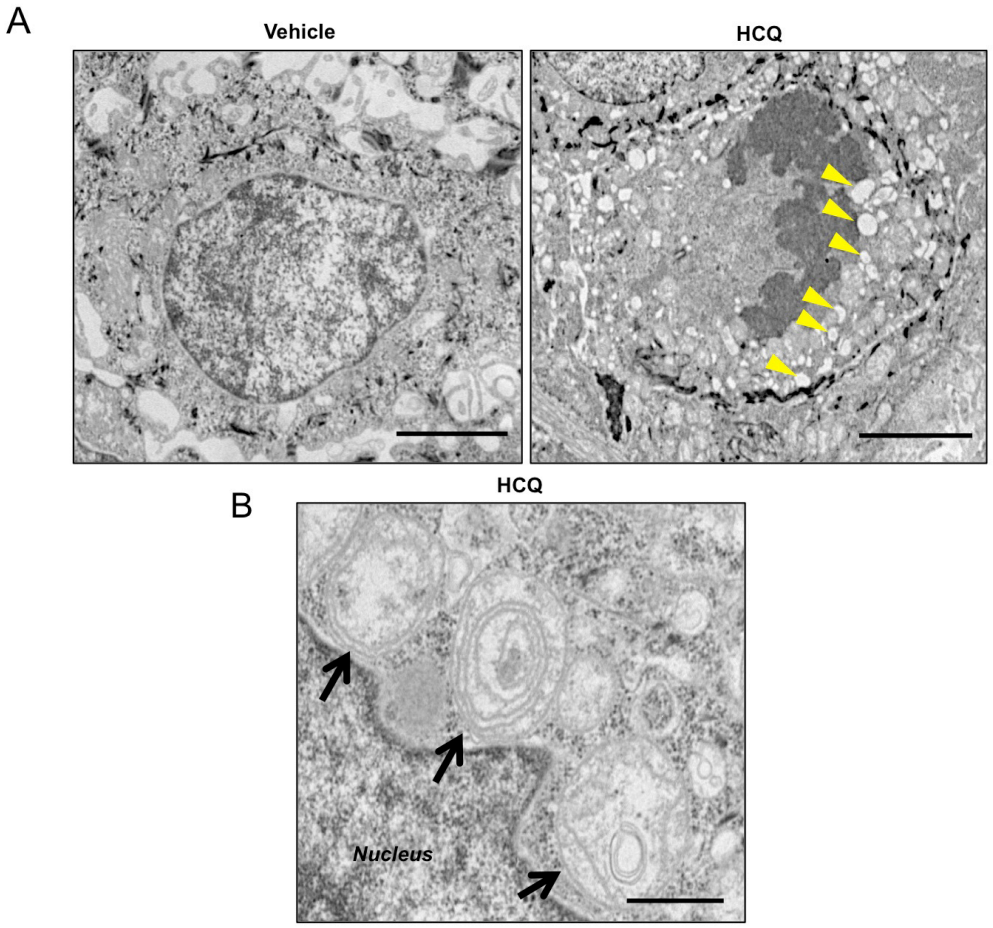

Supplementary Figure S2. Pharmacological autophagy inhibition promotes AV accumulation in TE11 xenograft tumors. Immunocompromised mice bearing established TE11 xenograft tumors were treated with vehicle control or HCQ (60 mg/kg) according to a 3 days on/2 days off schedule for 14 days. Tumors were then evaluated by TEM. (A) Representatives images of tumor cells from vehicle- or HCQ-treated mice. Arrowheads indicate Avs. Scale bars, 2 μm. (B) In tumors from HCQ-treated animals, multilamellar structures were detected within autophagic vesicles. Scale bar, 500 nm.

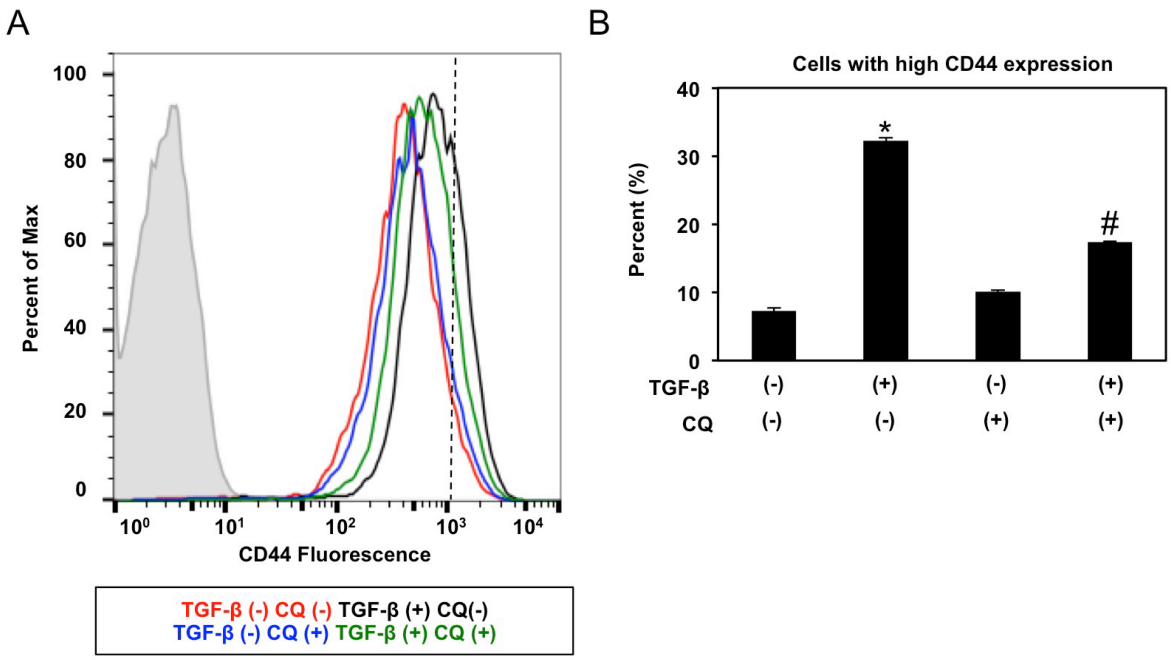

Supplementary Figure S3. Pharmacological autophagy inhibition suppresses TGF-β-mediated expansion of cells with high CD44 expression. TE11 cells were treated with TGF-β (5 ng/ml) and/or CQ (1 μg/ml) as indicated for 72 hours then assessed for CD44 expression via flow cytometry. (A) Representative flow cytometry histogram. Note cells with high CD44 expression are present to the right of the hatched line. (B) Bar diagram depicting average fold change in cells with high CD44 expression in each condition. *, $p<0.001$ vs. TGF-β (-) CQ (-). #, $p<0.05$ vs. TGF-β (+) CQ (-); (n=3); ANOVA with Tukey's post-hoc test.

A

Enrichment of biological processes associated with >2-fold upregulation EPC2T cells undergoing TGF-β-mediated EMT

Biological function	p value
Response to wound healing	1.36E-10
Blood vessel development	2.9E-10
Vascular development	5.54E-10
Inflammatory response	7.65E-10
Localization of cell	1.96E-09
Cell motility	1.96E-09
Cell migration	1.96E-09
Cellular component movement	2.92E-09
Angiogenesis	3.92E-09
Response to stress	5.95E-09

B

Enrichment of biological processes associated with >2-fold downregulation in EPC2T cells undergoing TGF-β-mediated EMT

Biological function	p value
Keratinocyte differentiation	2.48E-16
Epidermal cell differentiation	2.9E-16
Epidermis development	2.72E-15
Keratinization	8.06E-15
Epithelial cell differentiation	7.54E-14
Epithelium development	9.09E-10
Tissue development	2.40E-09
Regulation of peptidase activity	2.58E-05
Regulation of endopeptidase activity	8.32E-05
Negative regulation of peptidase activity	0.0001

Supplementary Figure S4. Influence of TGF-β on biological pathways in EPC2T cells. EPC2T cells were treated with TGF-β for 7 days then gene expression was evaluated by microarray analysis (GSE37994). Gene ontology analysis identified the top 10 significantly enriched biological processes for significantly upregulated (in A) and downregulated (in B) in comparison to a reference data set (Entrezgene_Protein coding) genes using the Gene SeT AnaLysis Toolkit. $p<0.05$ was considered significant.

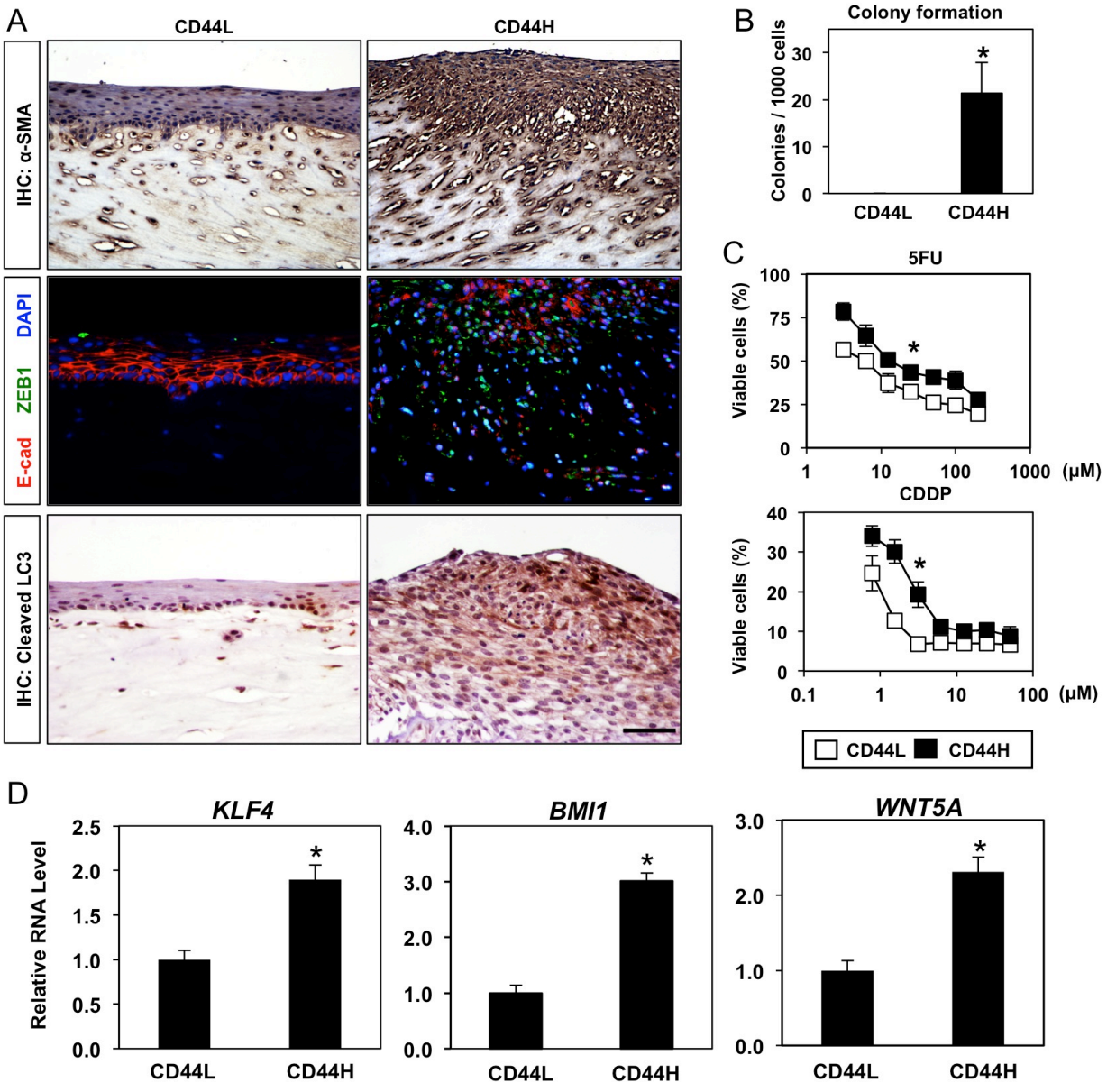

Supplementary Figure S5. CD44H EPC2T cells display properties consistent with EMT, enhanced malignant potential and expression of stem cell markers. Purified CD44L and CD44H, and unsorted EPC2T cells were analyzed. (A) Purified CD44L and CD44H cells were grown in organotypic 3D culture for IHC (α-SMA and cleaved LC3) or co-IF for E-cadherin (E-cad) and ZEB1 with representative images shown. Scale bars, 100 μm. DAPI visualizes nuclei in IF. (B) Purified CD44L and CD44H cells were subjected to soft agar colony formation assays for 3 weeks. *, $p<0.05$ vs. CD44L; (n=3). (C) Purified CD44L and CD44H cells were treated with indicated concentrations of 5-fluorouracil (5FU) or cisplatin (CDDP) for 72 hours then viability was evaluated by WST-1 assay. *, $p<0.05$ vs. CD44L; (n=3). (D) FACS-purified CD44L and CD44H EPC2T cells were evaluated for expression of indicated genes by quantitative RT-PCR. *, $p<0.05$ vs. CD44L; (n=3). Two-tailed Student's t-test (in B, D) or repeated measures ANOVA (in C) determined p values.

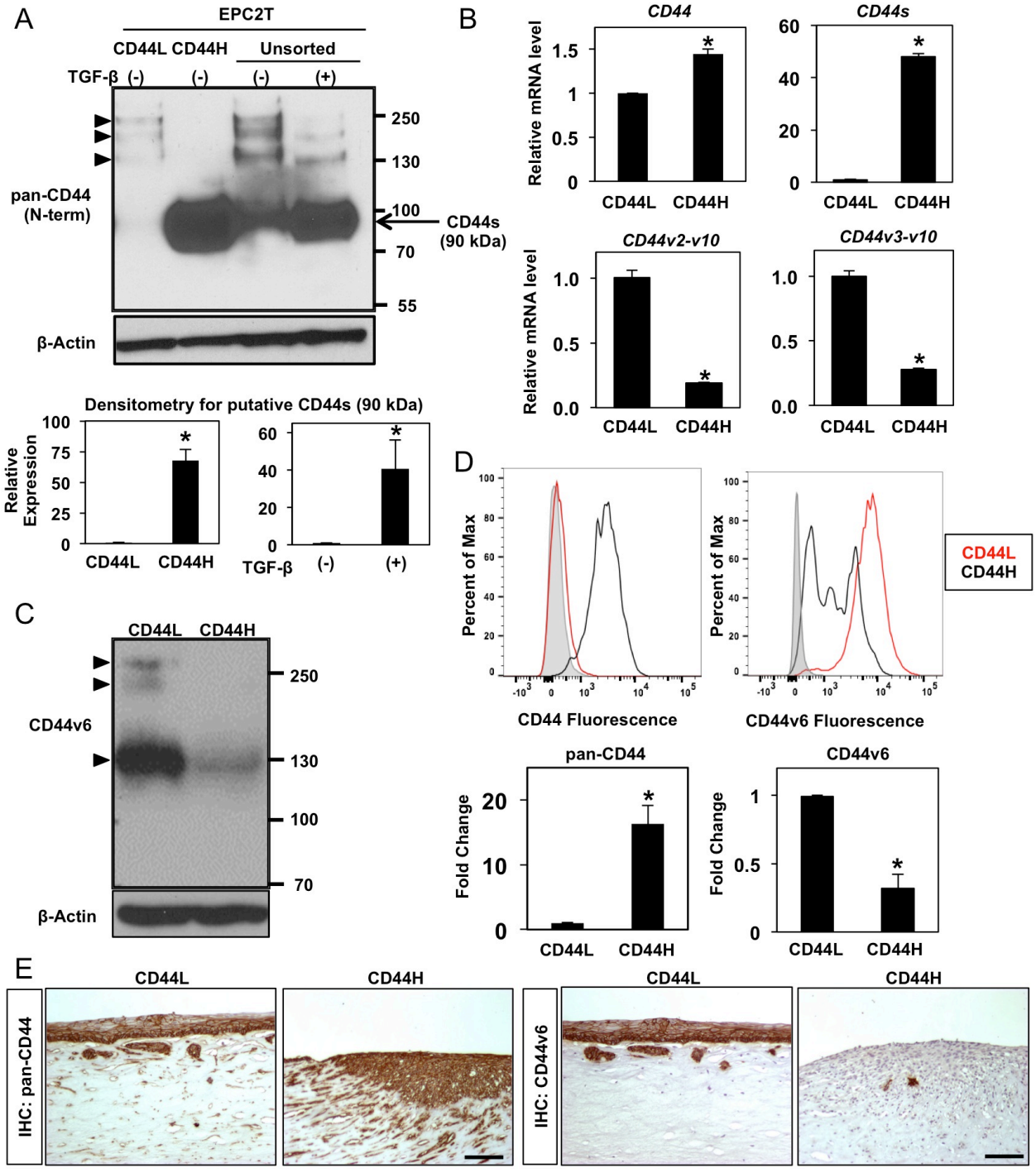

Supplementary Figure S6. Characterization of CD44 expression in EPC2T cells (A) FACS-purified and unsorted EPC2T cells were cultured in the presence or absence of TGF-β for 7 days for immunoblot analysis to assess CD44s (arrow, 90 kDa) and CD44v (arrowheads, ≥130 kDa) with β-Actin as a loading control. Densitometry was used to evaluate CD44s expression relative to β-Actin. *, $p<0.0001$ vs. CD44L; (n=3). (B) quantitative RT-PCR assessed mRNA expression of total *CD44* and indicated *CD44* isoforms in purified CD44L and CD44H EPC2T cells. *, $p<0.01$ vs. CD44L; (n=3). (C) CD44v6 expression (arrowheads, ≥130 kDa)was assessed in CD44L and CD44H cells by immunoblotting. (D) CD44 and CD44v6 protein level was assessed by flow cytometry with representative histograms and and relative fold changes shown. *, $p<0.05$ vs. CD44L; (n=3). (E) Purified CD44L and CD44H cells were grown in organotypic 3D culture for IHC (CD44, CD44v6) with representative images shown. Scale bars, 100 µm. Two-tailed Student's t-test was used to determine p values (in A, B, and D).

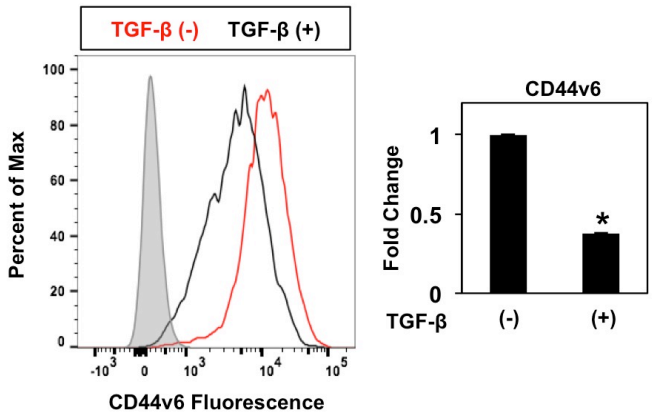

Supplementary Figure S7. CD44v6 downregulation in response to TGF-β FACS-purified CD44L EPC2T cells were cultured in the presence or absence of TGF-β for 7 days. Expression of CD44v6 protein was assessed by flow cytometry with representative histogram and and relative fold change shown. *, $p<0.001$; (n=3). Two-tailed Student's t-test was used to determine p value.

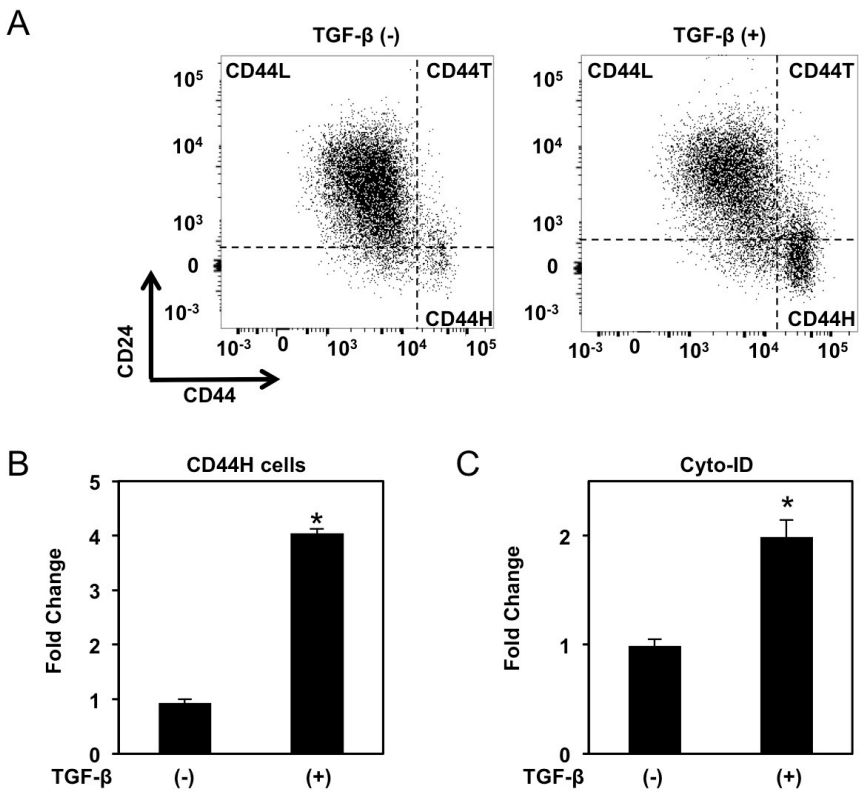

Supplementary Figure S8. TGF-β promotes CD44H cell generation and AV accumulation in transformed oral keratinocytes. FACS-purified CD44L OKF6T cells were cultured in the presence or absence of TGF-β (5 ng/ml) for 7 days. (A, B) Cells were analyzed for expression of CD24 and CD44 by flow cytometry to determine CD44H cells with representative dot plots (in A) and fold change (in B) shown. *, $p<0.0001$ vs. TGF-β (-); (n=3). (C) Flow cytometry determined Cyto-ID (geometric mean) with average fold change shown. *, $p<0.01$ vs. TGF-β (-); (n=3). Two-tailed Student's t-test determined p values (in B and C).

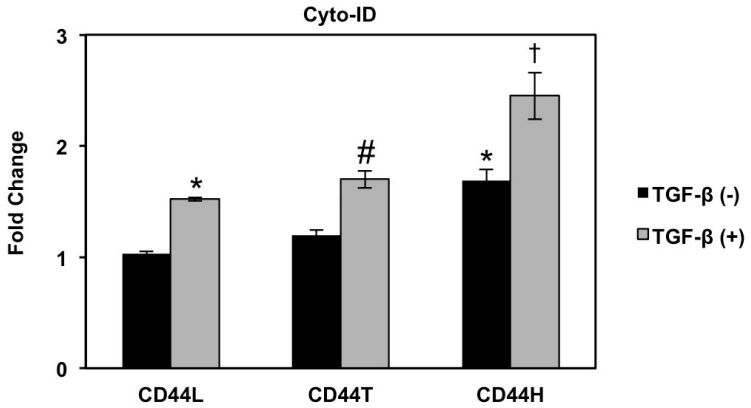

Supplementary Figure S9. Characterization of AV content in OKF6T subpopulations. OKF6T cells were cultured in the presence or absence of TGF-β (5 ng/ml) for 7 days. Using flow cytometry, cells were analyzed for CD24, CD44 and Cyto-ID. Bar diagram depicts relative Cyto-ID levels for each population (average geometric mean). *, $p<0.05$ vs. CD44L TGF-β (-); #, $p<0.05$ vs. CD44T TGF-β (-); †, VS. CD44H TGF-β (-); ANOVA with Tukey's post-hoc test; (n=3).

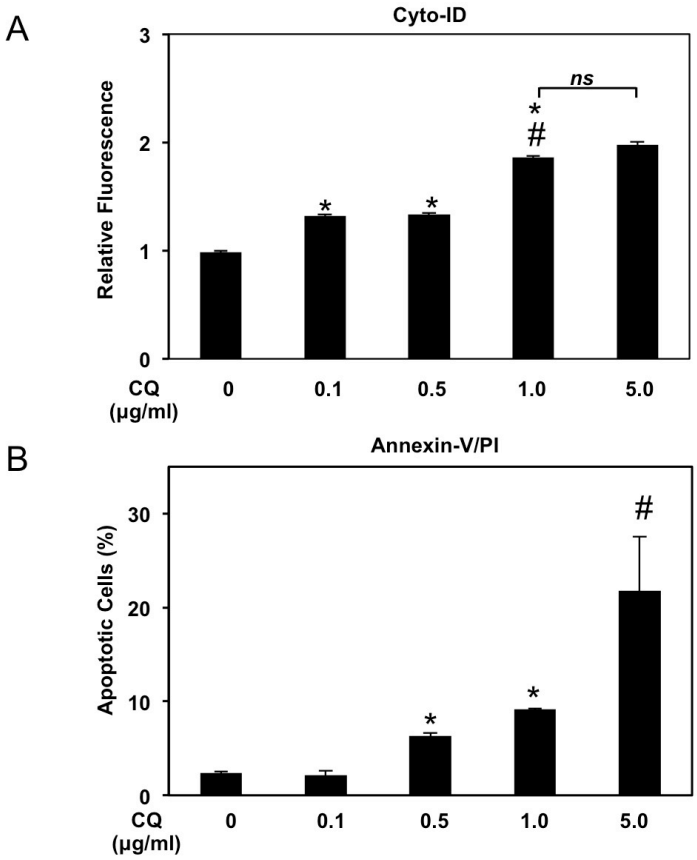

Supplementary Figure S10. Determination of optimal CQ concentration. EPC2T cells were cultured in the presence of indicated CQ concentrations for 14 days. (A) Flow cytometry for Cyto-ID was used to determine AV content. Bar diagram depicts relative Cyto-ID levels (average geometric mean) for each condition. *, $p<0.05$ vs. 0 µg/ml CQ; #, $p<0.05$ vs. 0.5 and 1.0 µg/ml CQ; *ns*, not significant. (n=3). (B) Annexin-V/PI flow cytometry was used to evaluate apoptosis with bar diagram depicting average percentage of early and late apoptotic cells (Annexin-V-positive PI-negative and Annexin-V-positive PI-positive) shown. *, $p<0.05$ vs. 0 µg/ml CQ; #, $p<0.05$ vs. 1.0 µg/ml CQ; (n=3). ANOVA with Tukey's post-hoc test determined p values (in A and B).

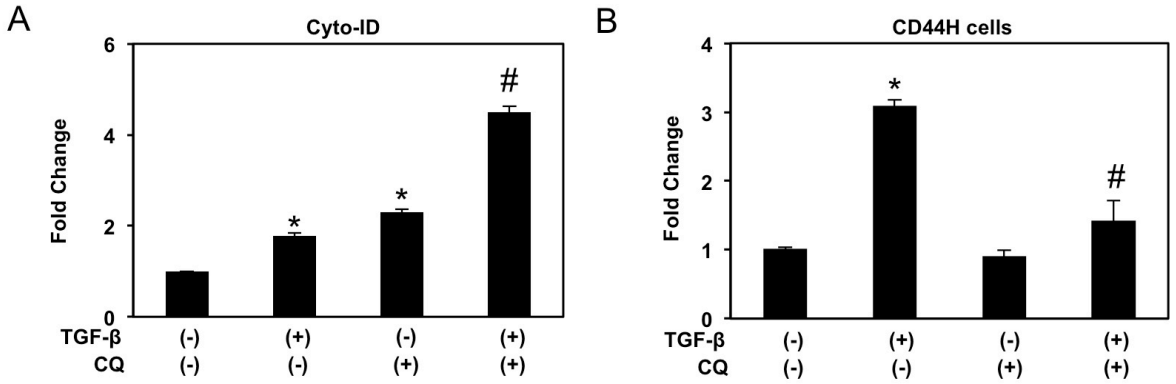

Supplementary Figure S11. Autophagy flux is activated during and required for EMT-mediated CD44H cell expansion in transformed oral keratinocytes. OKF6T cells were cultured in the presence or absence of TGF-β (5 ng/ml) and/or CQ (1 μg/ml) as indicated for 7 days. (A) Flow cytometry determined Cyto-ID with and relative Cyto-ID levels (average geometric mean) shown. *, $p<0.05$ vs. TGF-β (-) CQ (-); #, $p<0.05$ vs. TGF-β (+) CQ (-) and TGF-β (-) CQ (+); (n=3). (B) Cells were analyzed for expression of CD24 and CD44 by flow cytometry to determine CD44H cells with relative fold change shown *, $p<0.05$ vs. TGF-β (-) CQ (-); #, $p<0.05$ vs. TGF-β (+) CQ (-) and TGF-β (-) CQ (+); (n=3). ANOVA with Tukey's post-hoc test determined p values (in A and B).

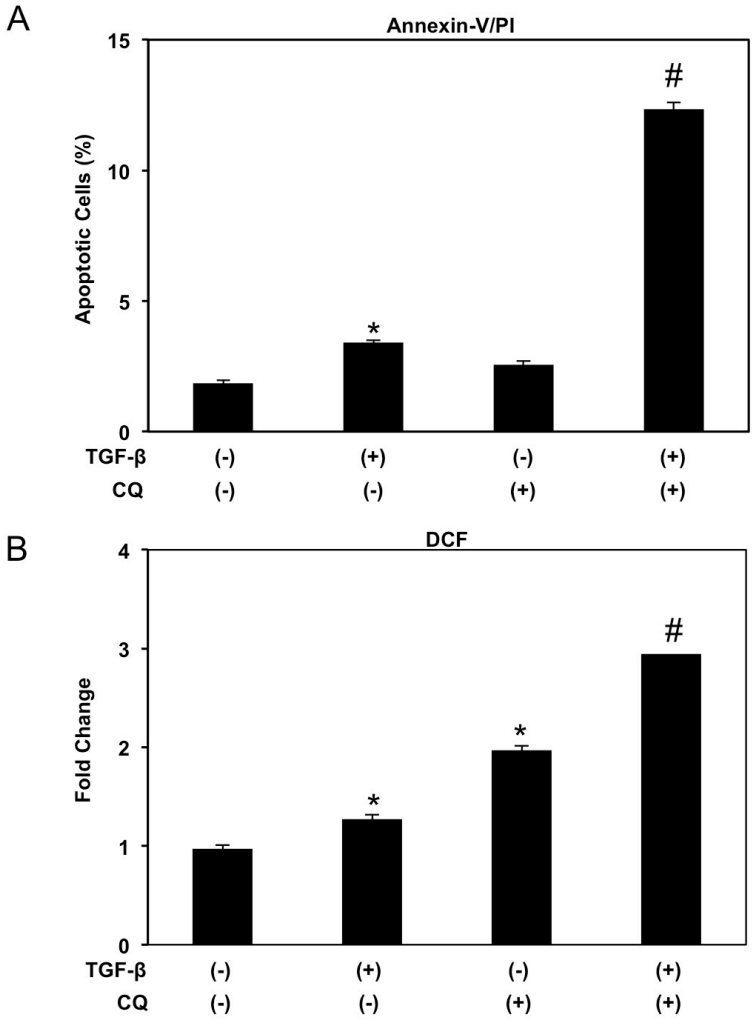

Supplementary Figure S12. Autophagy inhibition in oral keratinocytes undergoing CD44H cell generation promotes cell death and oxidative stress. OKF6T cells were cultured in the presence or absence of TGF-β (5 ng/ml) and/or CQ (1 μg/ml) for 14 days. (A) Flow cytometry for Annexin-V/PI was used to evaluate apoptosis with bar diagram depicting average percentage of early (Annexin-V-positive PI-negative) and late (Annexin-V-positive PI-positive) apoptotic cells shown. *, $p<0.05$ vs. TGF-β (-) CQ (-); #, $p<0.05$ vs. TGF-β (+) CQ (-) and TGF-β (-) CQ (+); (n=3). (B) Reactive oxygen species were evaluated by DCF flow cytometry with and relative fluorescence levels (average geometric mean) shown. *, $p<0.05$ vs. TGF-β (-) CQ (-); #, $p<0.05$ vs. TGF-β (+) CQ (-) and TGF-β (-) CQ (+); (n=3). ANOVA with Tukey's post-hoc test determined p values (in A and B).

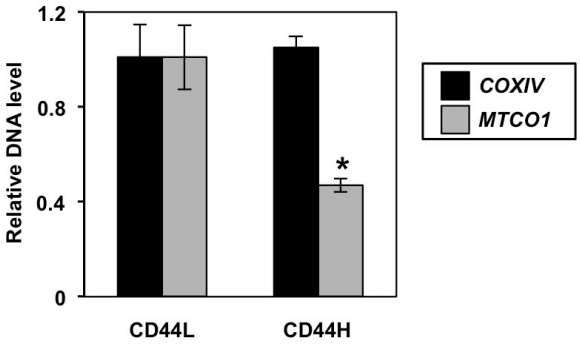

Supplementary Figure S13. Established CD44H cells display decreased mtDNA content. Early passage FACS-purified CD44L and CD44H EPC2T cells were evaluated for mtDNA content by PCR. Note that *MTCO1* is encoded by mitochondrial DNA while *COXIV* is encoded by nuclear DNA. Gene expression is presented relative to an internal control nuclear encoded *GAPDH*. *, $p<0.05$ vs. MTCO1 in CD44L; two-tailed Student's t-test; (n=3).

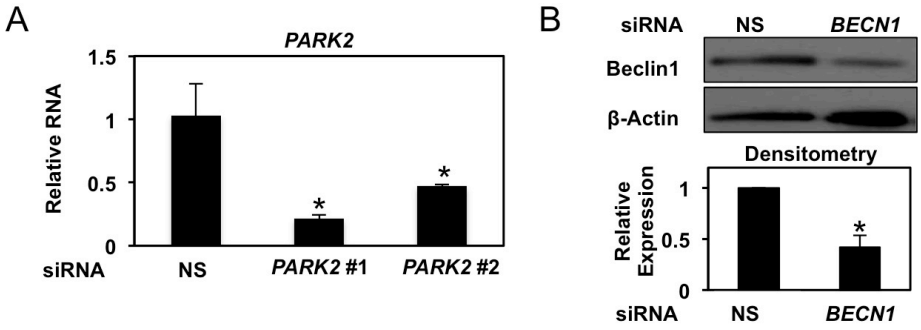

Supplementary Figure S14. Confirmation of siRNA-mediated depletion of Parkin or Beclin1. (A) EPC2T cells were transfected with two siRNA sequences targeting *PARK2* or a non-silencing control sequence. 72 hours following transfection, cells were subjected to qRT-PCR analysis for *PARK2*. Gene expression is presented relative to an internal loading control (*ACTB*). *, $p<0.05$ vs. NS; ANOVA with Tukey's post-hoc test; (n=3). (B) EPC2T cells were transfected with an siRNA sequence targeting BECN1 or a non-silencing (NS) control sequence. 72 hours following transfection, cells were subjected to immunoblot analysis for Beclin1. β-Actin serves as a loading control. Densitometry determined level of Beclin1 relative to β-Actin . *, $p<0.005$ vs. NS; two-tailed Student's t-test; (n=3).